PbS as a Highly Catalytic Counter Electrode for Polysulfide-Based Quantum Dot Solar Cells

ARTICLE *in* THE JOURNAL OF PHYSICAL CHEMISTRY C · MARCH 2011

Impact Factor: 4.77 · DOI: 10.1021/jp112010m

6 AUTHORS, INCLUDING:

Zion Tachan
Bar Ilan University
13 PUBLICATIONS **596** CITATIONS
SEE PROFILE

Menny Shalom
Max Planck Institute of Colloids and Interfaces
37 PUBLICATIONS **1,878** CITATIONS
SEE PROFILE

Sven Rühle
Xjet 3D
47 PUBLICATIONS **2,391** CITATIONS
SEE PROFILE

Arie Zaban
Bar Ilan University
170 PUBLICATIONS **10,728** CITATIONS
SEE PROFILE

THE JOURNAL OF PHYSICAL CHEMISTRY C

ARTICLE

pubs.acs.org/JPCC

PbS as a Highly Catalytic Counter Electrode for Polysulfide-Based Quantum Dot Solar Cells

Zion Tachan, Menny Shalom, Idan Hod, Sven Rühle, Shay Tirosh, and Arie Zaban*

Institute of Nanotechnology & Advanced Materials, Department of Chemistry, Bar Ilan University, 52900 Ramat Gan, Israel

Supporting Information

ABSTRACT: We show that a significant improvement of the light to electric power conversion efficiency of quantum dot sensitized solar cells with a polysulfide electrolyte can be achieved when a PbS counter electrode is used. An acid pretreatment of a Pb metal foil followed by dipping into polysulfide solution provides a counter electrode which improves the short circuit current, open circuit voltage, and fill factor compared to commonly used Pt electrodes. Electrochemical impedance spectroscopy reveals a low charge transfer resistance between polysulfide and PbS, indicating the high catalytic activity of PbS. Moreover, a comparison with reported charge transfer resistance values at open circuit potential for alternative counter electrodes for polysulfide shows that PbS is the most catalytic of all. For a CdSe quantum dot sensitized mesoporous TiO_2 electrode, we achieved a conversion efficiency of 3% using PbS as a counter electrode.

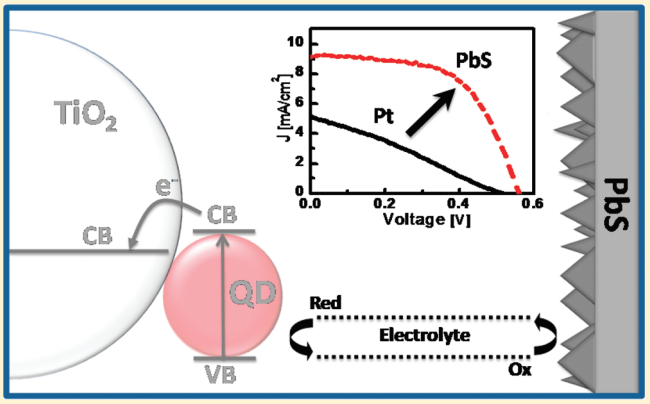

INTRODUCTION

Dye-sensitized solar cells (DSSC) have attracted tremendous attention as a potential low-cost alternative for single or polycrystalline p−n junction silicon solar cells.[1−3] DSSCs are based on a mesoporous TiO_2 film, covered with a dye monolayer that is immersed into an I^-/I_3^- redox electrolyte while the electric circuit is closed by a transparent conducting oxide (TCO) front electrode and a Pt counter electrode (Pt-CE). Different shapes and geometries such as curved surfaces and tubes[4] have been studied allowing self-light tracking and waveguide integration.[5] Conversion efficiencies around 11% have been reported using a ruthenium complex as the sensitizer, which has an absorption onset around 750 nm.[6] Extensive research has been dedicated to the synthesis of new dyes with an onset at longer wavelengths in order to increase the photocurrent and subsequently the cell efficiency.[7]

As an alternative to dye molecules, semiconductor quantum dots (QDs) such as CdS,[8−10] CdSe,[8,11,12] PbS,[13] InAs,[14] InP,[15] and others[16] as well as extremely thin inorganic absorber layers[17,18] have been used. QDs are very attractive because of their size dependent optical band gap,[11] the possibility to design hierarchical multilayer absorber structures,[18,19] and the potential to use them for multiexciton generation from a single photon.[20] However, most QDs suffer from photodegradation when used in conjunction with the I^-/I_3^- redox couple.[21] Consequently, quantum dot sensitized solar cells (QDSCs) are often based on aqueous polysulfide electrolyte with minor use of the $Fe(CN)_6^{3-}/Fe(CN)_6^{4-}$ couple[22] and various Co-based electrolytes.[23]

Pt, being a catalytic electrode for organic I^-/I_3^- redox electrolyte, is the most widespread counter electrode (CE) in DSSCs showing low charge transfer resistance, R_{ct}, at the CE/electrolyte interface. However, in conjunction with aqueous polysulfide electrolytes, Pt and other novel metals like Au are not very catalytic, generating considerable overpotentials for the electrolyte regeneration which is reflected in a reduction of the total conversion efficiency of the solar cell. Alternative CE materials for polysulfide solution have been investigated such as CoS, Cu_2S, NiS, Au, and carbon.[24−33] Low catalytic activities were observed for carbon, Au, and Pt, followed by NiS, while the best results were obtained for CoS and Cu_2S. Short- and long-term stability measurements in the presence of a photoanode indicated that CoS and Cu_2S electrodes may contaminate the electrolyte and subsequently the photoanode.[25] PbS that was prepared by electroplating showed a catalytic activity similar to that of CoS and Cu_2S but with an inferior long-term stability.[25]

In this work we have developed a new and simple fabrication method for a highly catalytic PbS counter electrode (PbS-CE) that involves the formation of $PbSO_4$ as an intermediate state. X-ray diffraction spectroscopy and high-resolution scanning electron microscopy were used to characterize the morphology of the PbS electrode. Impedance spectroscopy was applied to derive R_{ct} values for the PbS/polysulfide and Pt/polysulfide

Received: December 17, 2010
Revised: February 28, 2011
Published: March 15, 2011

dx.doi.org/10.1021/jp112010m | J. Phys. Chem. C 2011, 115, 6162–6166

systems for comparison. A CdSe QD-sensitized photoelectrode was used in conjunction with an aqueous polysulfide electrolyte and the PbS-CE to record $I-V$ measurements under illumination and to compare the solar cell performance to a cell with a Pt-CE. Our results show that the PbS-CE reported here provides better performance while bypassing contamination problems known from alternative materials.

EXPERIMENTAL SECTION

PbS Counter Electrode Preparation and Characterization. Pb metal foil was purchased from Alfa Aesar (99.998% metal basis). As a pretreatment the foil was polished with sand paper, washed with deionized water, and immersed into concentrated H_2SO_4 solution (water−acid volume ratio 1:1) for 24 h at room temperature and afterward washed with deionized water. The pretreatment changed the color of the appearance of the foil from shiny metal to gray. Subsequently, the foil was inserted into a polysulfide solution (1 M Na_2S, 0.1 M sulfur, and 0.1 M NaOH dissolved in deionized water) for 24 h before it was rinsed with deionized water and dried in an air stream. This treatment changed the appearance of the foil from gray to dark black. Heating the H_2SO_4 solution can speed up the pretreatment without affecting the CE performance.

X-ray diffraction (XRD) measurements were performed with a Bruker D8 X-ray diffractometer (Cu Kα radiation, λ = 1.5406 Å) using the database JCP2: 01-087-0663, JCP2: 01-078-1901, and JCP2: 01-072-2102 for peak identification. High-resolution scanning electron microscopy (HR-SEM) images were recorded with a FEI, Helios NanoLab 600i dual beam.

Electrochemical impedance spectroscopy (EIS) was carried out in the dark with a Princeton PARSTAT 2273 using Ag/AgCl (in aqueous KCl 3M) as a reference electrode. ZSIM software was used to derive R_{ct} from a frequency scan (100 kHz−10 mHz, 10 mV amplitude) at a given dc bias (0.5−1.0 V vs Ag/AgCl).

Photoelectrode Preparation. The fluorine-doped tin oxide (FTO) purchased from Pilkington (8 Ω/square) was cleaned with ethanol and mild soap, thoroughly rinsed with deionized water, and dried in a filtered dry air stream. Commercial TiO_2 paste (Ti-Nanoxide D, Solaronix, Switzerland) was spread by the doctor blade technique, dried, and sintered at 450 °C for 30 min. The mesoporous film thickness was 4.5 μm, measured by a profilometer (Surftest SV-500).

A seeding layer of CdS was deposited by the SILAR method[34] prior to the CdSe sensitization. Therefore, the TiO_2 electrodes were dipped into 0.1 M $Cd(ClO_4)_2$ for 1 min, washed with deionized water, immersed into 0.1 M Na_2S aqueous solution, and washed again. After seeding, chemical bath deposition (CBD) was used to sensitize the electrode with CdSe QDs following the procedure by Gorer and Hodes.[8] Sodium selenosulphate (Na_2SeSO_3) solution (80 mM) was prepared by dissolving Se powder in a 200 mM Na_2SO_3 solution (solution A). $CdSO_4$ (80 mM) and trisodium salt of nitrilotriacetic acid ($N(CH_2COONa)_3$) (120 mM) were mixed in a 1:1 volume ratio (solution B), before solution A and B were mixed in a 1:2 volume ratio. The mesoporous TiO_2 electrodes were immersed into the final solution for 30 h at 10 °C and kept in the dark. Finally the ZnS coating was applied by dipping the electrode into a 0.1 M $Zn(CH_3COO)_2$ solution (30 s), rinsing with deionized water, dipping it into 0.1 M Na_2S solution (30 s), and rinsing it again.[35]

Solar Cell Characterization. Current−potential ($I-V$) measurements were performed with an Eco-Chemie potentiostat with a scan rate of 10 mV/s using a sandwich cell configuration. Aqueous polysulfide electrolyte consisting of 1 M sodium sulfide (Na_2S), 0.1 M sulfur, and 0.1 M sodium hydroxide (NaOH) was used as a redox electrolyte. To ensure reproducible measurements, the distance between the counter and working electrode was kept constant for all measurements, using a glass microscope slide as a mechanical support for the relatively soft Pb/PbS foil. A 250 W xenon arc lamp (Oriel) calibrated to 100 mW/cm^2 served as a light source. The illuminated area of the cell was 0.64 cm^2. Incident photon to current efficiency (IPCE) measurements was performed employing a 250 W xenon lamp with a monochromator and Keithley controlled by a computer. For comparison also a Platinized CE was used where Pt particles (Platisol) were drop-casted onto FTO glass followed by annealing (400 °C, 5 min).

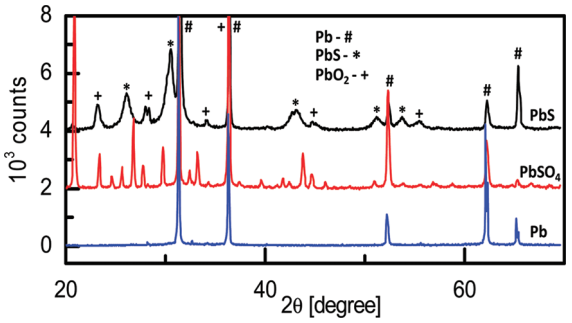

Figure 1. XRD spectra of the untreated Pb metal foil (bottom), after H_2SO_4 treatment (middle), and finally after polysulfide treatment (top) showing the PbS evolution. For better visibility the spectra in the middle and top were offset by 2000 and 4000 counts, respectively.

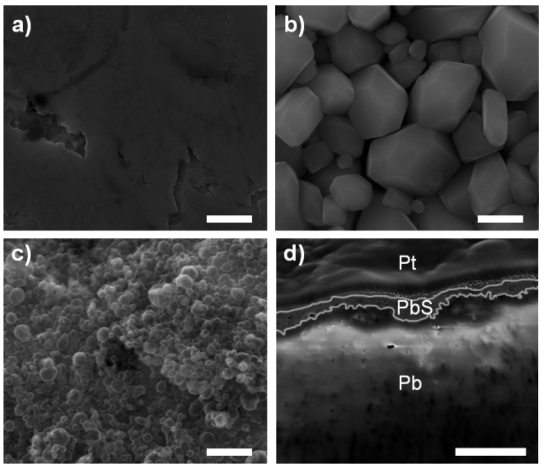

Figure 2. HRSEM images of (a) the Pb foil before any treatment, (b) after immersion into concentrated H_2SO_4 solution for 24 h, and (c) after subsequent treatment with polysulfide solution. (d) Cross section produced with a focused ion beam (FIB). Prior to the ion milling, a thin layer of Pt was deposited on top of the PbS layer to improve the quality of the cross section and subsequently the image. The Pt/PbS and PbS/Pb interfaces are highlighted by a gray line for better visibility. The scale bar in all figures represents a length of 1 μm.

RESULTS AND DISCUSSION

PbS counter electrode (PbS-CE) prepared by the H_2SO_4 pretreatment was characterized by XRD (Figure 1). The bottom

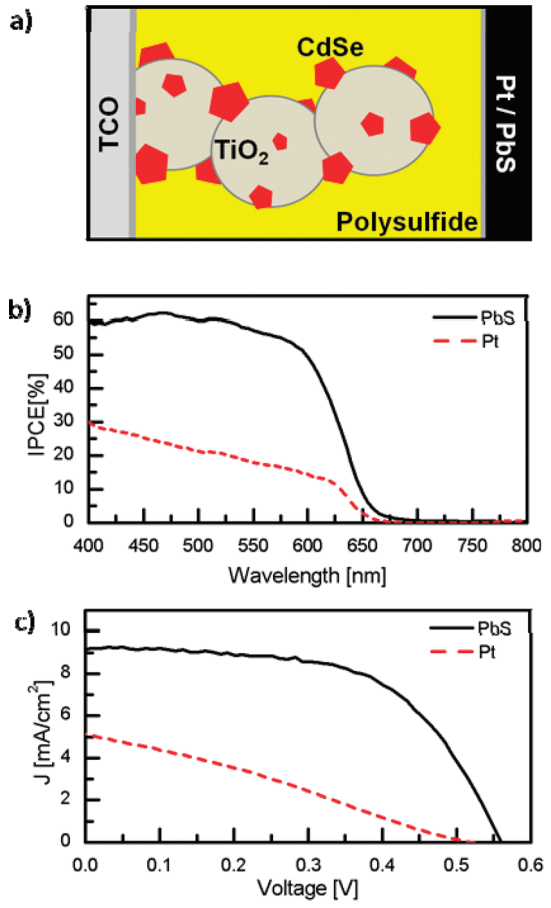

Figure 3. Characterizations of CdSe QDSC based on PbS and standard Pt counter electrodes (solar cell active area is 0.64 cm^2): (a) schematic structure of the CdSe QDSC; (b) IPCE measurement; (c) $I-V$ curve characteristics, under one sun illumination.

graph shows the diffraction pattern of the Pb foil before any treatment, and the strong peaks can be attributed to the face-centered cubic structure of Pb metal. The graph in the middle shows a number of new peaks that appear after the H_2SO_4 treatment which are due to the formation of $PbSO_4$. These peaks disappear after the immersion of the acid-treated Pb foil into polysulfide solution (upper graph in Figure 1), and new peaks appear at 2θ = 26.1°, 30.5°, 43.0°, 51.3°, and 53.7°, which are characteristic for the formation of PbS. The Pb peaks remain visible in all graphs because the Pb foil is only converted within a thin surface layer with a thickness below the penetration depth of the X-rays. The PbS peaks are much broader compared to the Pb, indicating that the PbS is polycrystalline with a rather small crystal size. The strong peaks at 2θ = 23.2°, 28.5°, 34.1°, 45.0°, and 55.5° (upper graph) belong to the orthorhombic structure of the α-PbO_2 phase.

High-resolution SEM images of the PbS electrode formation show the smooth surface of the Pt foil before treatment (Figure 2a). After immersion into H_2SO_4, micrometer-sized crystals of $PbSO_4$ are formed, which leads to a substantial increase of the electrode's surface area (Figure 2b). The subsequent treatment with polysulfide solution converts the $PbSO_4$ into small PbS crystals with a diameters in the submicrometer regime (Figure 2c). PbO_2 crystals might also be present at the surface; however, they cannot be distinguished in the HRSEM

Table 1. Photovoltaic Properties of CdSe QDSC Showing the Significant Improvement Achieved by Using PbS-CE in This Type of Cell[a]

counter in use	efficiency (%)	V_{oc} (mV)	J_{sc} (mA/cm^2)	fill factor
PbS	3.01	554	9.28	58.8
Pt	0.75	514	5.20	28.2

[a] Error estimation is approximately 1%.

images from PbS. PbO_2 is not catalytic to the polysulfide electrolyte. Consequently, its presence decreases the overall catalytic activity of the counter electrode. However, the preparation method used in this work ensures that the fraction of PbO_2 at the electrode surface is very small compared with the active surface of the PbS.

A cross section of the PbS-CE (Figure 2d) reveals a PbS layer thickness ranging from 70 to 350 nm. The acid treatment is an efficient method to increase the surface area and to provide a large number of catalytic sites which enhance the charge transfer kinetics at the polysulfide/PbS CE interface in an operating solar cell. Moreover, the ease of PbS-CE fabrication is a fundamental advantage of the presented method.

CdSe-sensitized QDSCs were electrically characterized by incident photon to current efficiency (IPCE) and $I-V$ measurements to demonstrate the excellent performance of PbS as a CE for polysulfide electrolyte. A schematic structure of the CdSe QDSC is depicted in Figure 3a. Upon illumination, photons are absorbed by the QDs generating excitons, followed by electron injection into the TiO_2 conduction band and hole transfer into the electrolyte. Charge collection at the TCO front electrode and at the PbS or Pt counter electrode is diffusion driven. The IPCE measurements presented in Figure 3b show the significant improvement in charge collection associated with the exchange of the CE from Pt to PbS. Having similar spectral response (photocurrent onset), the charge collection efficiency at the cell utilizing the PbS is around 55% compared with 20% for the Pt CE analogue. The $I-V$ measurements of the CdSe QDSC shown in Figure 3c for both CEs show the same trend. One can see that the use of PbS as a CE significantly improved the short circuit current density (J_{sc}) and the open circuit voltage (V_{oc}) and strongly increased the fill factor such that a fourfold increase of the light to electric power conversion efficiency up to 3.0% is achieved (see also Table 1). Significant improvement in charge transfer at the CE/electrolyte interface reduces internal resistances, recombination rates, and concentration gradients in the electrolyte, parameters that strongly affect J_{sc} and the fill factor.

The fast charge transfer at the PbS/electrolyte interface causes a change in the ions' concentration in the solution and by that influence the recombination rates at the working electrode/electrolyte interface. The relatively small increase of V_{oc} seems to be the result of a more positive potential of the catalytic PbS in the electrolyte. Consequently the measured improvement in all cell parameters upon introduction of the PbS CE to the cell is a strong indication for an enhanced catalytic activity of the PbS in conjunction with the polysulfide electrolyte. Stability tests of the PbS counter electrode performed under illumination for over 100 h show no degradation (see Supporting Information image 2).

Impedance spectroscopy measurements were performed with a standard three-electrode configuration using Ag/AgCl as reference electrode to derive the charge transfer resistance between the CE and the polysulfide electrolyte. The impedances

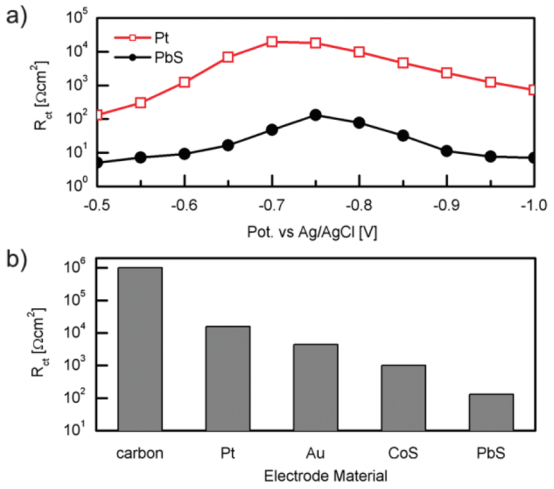

Figure 4. (a) Charge transfer resistance of a PbS or Pt electrode in aqueous polysulfide electrolyte, measured in a three-electrode cell configuration using Ag/AgCl as a reference electrode (measurement inaccuracy <0.4%). (b) Comparison of R_{ct} measured at the open circuit potential for different electrode materials showing the lowest value for the PbS electrode. R_{ct} values for carbon, Au, and CoS were taken from refs 26 and 34.

of two symmetric cells[28,36] composed of a working and CE both from PbS or Pt were measured in the dark as a function of an applied bias (−0.5 to −1.0 V vs Ag/AgCl). At each potential, a full frequency scan from 100 kHz to 10 mHz was performed. The charge transfer resistance, R_{ct}, corresponding to the charge exchange between the PbS or Pt working electrodes and the polysulfide electrolyte was derived from the semiarcs in the Nyquist plots. At an applied potential of around −0.73 V vs Ag/AgCl, the charge transfer resistance has a maximum of 130 Ω cm^2 for the PbS-CE electrode, while R_{ct} of the Pt-CE is, with 19 700 Ω cm^2, more than 2 orders of magnitude larger (Figure 4a). The measured open circuit potentials in the dark, −0.71 V for the Pt and −0.75 V for the PbS electrode, roughly match the redox potential of the polysulfide electrolyte. A comparison with previously reported R_{ct} values measured at the open circuit potential for different CE materials (carbon, Au, and CoS)[28,36] is presented in Figure 4b, which clearly shows the high catalytic activity and thus the superiority of PbS as a CE for aqueous polysulfide electrolyte. The R_{ct} value of 130 Ω cm^2 for PbS is the lowest reported R_{ct} value up to date, even beating the performance of Au and CoS, which gave better results than Pt.

CONCLUSION

We have characterized PbS as a highly catalytic counter electrode (CE) for aqueous polysulfide electrolyte. In conjunction with a CdSe QD-sensitized photoelectrode, light to electric power conversion efficiencies of 3.0% were reached while the same photoelectrode together with a Pt-CE was not able to convert more than 0.8% of the solar energy into electrical power. With a PbS-CE it was possible to reach a fill factor close to 60% and a photocurrent density above 9 mA/cm^2, while high incident photon to current efficiencies above 55% were reached over a broad spectral range. Comparison with alternative CE materials such as Pt, Au, or CoS shows that PbS has the lowest charge transfer resistance at O_{cp}, which was derived from electrochemical impedance spectroscopy in polysulfide electrolyte. Highly catalytic counter electrodes are a prerequisite for further improvement of the conversion efficiency of polysulfide electrolyte based QDSCs.

ASSOCIATED CONTENT

Supporting Information. The catalytic behavior of the PbS is evident in various polysulfide-based solar cells. An example utilizing CdS is provided including preparation and characterization of the CdS-sensitized electrodes, $I-V$ curve, and IPCE. In addition, stability tests of CdSe anode using PbS as counter electrode are presented as well. This material is available free of charge via the Internet at http://pubs.acs.org.

AUTHOR INFORMATION

Corresponding Author
*E-mail address: zabana@mail.biu.ac.il.

ACKNOWLEDGMENT

The authors thank The Israel Science Foundation for the financial support of this study. S.R. acknowledges the support of the European Union within the FP7 framework (Marie Curie Intra-European Fellowship for Career Development).

REFERENCES

(1) O'Regan, B.; Grätzel, M. *Nature* **1991**, *353*, 737–740.
(2) Gratzel, M. *J Photochem. Photobiol., C: Photochem. Rev.* **2003**, *4*, 145–153.
(3) Peter, L. M. *J. Phys. Chem. C* **2007**, *111*, 6601–6612.
(4) Tachan, Z.; Ruhle, S.; Zaban, A. *Sol. Energy Mater. Sol. Cells* **2010**, *94*, 317–322.
(5) Ruhle, S.; Greenwald, S.; Koren, E.; Zaban, A. *Opt. Express* **2008**, *16*, 21801–21806.
(6) Cao, Y. M.; Bai, Y.; Yu, Q. J.; Cheng, Y. M.; Liu, S.; Shi, D.; Gao, F. F.; Wang, P. *J. Phys. Chem. C* **2009**, *113*, 6290–6297.
(7) Matar, F.; Ghaddar, T. H.; Walley, K.; DosSantos, T.; Durrant, J. R.; O'Regan, B. *J. Mater. Chem.* **2008**, *18*, 4246–4253.
(8) Gorer, S.; Hodes, G. *J. Phys. Chem.* **1994**, *98*, 5338–5346.
(9) Shalom, M.; Ruhle, S.; Hod, I.; Yahav, S.; Zaban, A. *J. Am. Chem. Soc.* **2009**, *131*, 9876-+.
(10) Hodes, G.; Howell, I. D. J.; Peter, L. M. *J. Electrochem. Soc.* **1992**, *139*, 3136–3140.
(11) Kamat, P. V. *J. Phys. Chem. C* **2008**, *112*, 18737–18753.
(12) Kongkanand, A.; Tvrdy, K.; Takechi, K.; Kuno, M.; Kamat, P. V. *J. Am. Chem. Soc.* **2008**, *130*, 4007–4015.
(13) Lee, H. J.; Chen, P.; Moon, S. J.; Sauvage, F.; Sivula, K.; Bessho, T.; Gamelin, D. R.; Comte, P.; Zakeeruddin, S. M.; Il Seok, S.; Grätzel, M.; Nazeeruddin, M. K. *Langmuir* **2009**, *25*, 7602–7608.
(14) Yu, P. R.; Zhu, K.; Norman, A. G.; Ferrere, S.; Frank, A. J.; Nozik, A. J. *J. Phys. Chem. B* **2006**, *110*, 25451–25454.
(15) Zaban, A.; Micic, O. I.; Gregg, B. A.; Nozik, A. J. *Langmuir* **1998**, *14*, 3153–3156.
(16) Ruhle, S.; Shalom, M.; Zaban, A. *Chemphyschem* **2010**, *11*, 2290–2304.
(17) Herzog, C.; Belaidi, A.; Ogacho, A.; Dittrich, T. *Energy Environ. Sci.* **2009**, *2*, 962–964.
(18) Moon, S. J.; Itzhaik, Y.; Yum, J. H.; Zakeeruddin, S. M.; Hodes, G.; Grätzel, M. *J. Phys. Chem. Lett.* **2010**, *1*, 1524–1527.
(19) Shalom, M.; Albero, J.; Tachan, Z.; Martinez-Ferrero, E.; Zaban, A.; Palomares, E. *J. Phys. Chem. Lett.* **2010**, *1*, 1134–1138.
(20) Nozik, A. J. *Nano Lett.* **2010**, *10*, 2735–2741.
(21) Shalom, M.; Dor, S.; Rühle, S.; Grinis, L.; Zaban, A. *J. Phys. Chem. C* **2009**, *113*, 3895–3898.

(22) Tachibana, Y.; Umekita, K.; Otsuka, Y.; Kuwabata, S. *J. Phys. D: Appl. Phys.* **2008**, 41.
(23) Hyo Joong, L.; Jun-Ho, Y.; Leventis, H. C.; Zakeeruddin, S. M.; Haque, S. A.; Chen, P.; Sang, S.; Il, M.; Gratzel; Nazeeruddin, M. K. *J. Phys. Chem. C* **2008**, *112*, 11600–11608.
(24) Hodes, G.; Manassen, J.; Cahen, D. *J. Appl. Electrochem.* **1977**, *7*, 181–182.
(25) Hodes, G.; Manassen, J.; Cahen, D. *J. Electrochem. Soc.* **1980**, *127*, 544–549.
(26) Yu, Z. R.; Du, J. H.; Guo, S. H.; Zhang, H. Y.; Matsumoto, Y. *Thin Solid Films* **2002**, *415*, 173–176.
(27) Gimenez, S.; Mora-Sero, I.; Macor, L.; Guijarro, N.; Lana-Villarreal, T.; Gomez, R.; Diguna, L. J.; Shen, Q.; Toyoda, T.; Bisquert, J. *Nanotechnology* **2009**, 20.
(28) Mora-Sero, I.; Gimenez, S.; Fabregat-Santiago, F.; Gomez, R.; Shen, Q.; Toyoda, T.; Bisquert, J. *Acc. Chem. Res.* **2009**, *42*, 1848–1857.
(29) Esposito, D. V.; Dobson, K. D.; McCandless, B. E.; Birkmire, R. W.; Chen, J. G. *J. Electrochem. Soc.* **2009**, *156*, 962–969.
(30) Fan, S. Q.; Fang, B.; Kim, J. H.; Kim, J. J.; Yu, J. S.; Ko, J. *Appl. Phys. Lett.* **2010**, 96.
(31) Kiyonaga, T.; Akita, T.; Tada, H. *Chem. Commun. (Cambridge, U.K.)* **2009**, 2011–2013.
(32) Yang, Z.; Chen, C.-Y.; Liu, C.-W.; Chang, H.-T. *Chem. Commun. (Cambridge, U.K.)* **2010**, *46*, 5485–5487.
(33) Zhang, Q. X.; Zhang, Y. D.; Huang, S. Q.; Huang, X. M.; Luo, Y. H.; Meng, Q. B.; Li, D. M. *Electrochem. Commun.* **2010**, *12*, 327–330.
(34) Vogel, R.; Pohl, K.; Weller, H. *Chem. Phys. Lett.* **1990**, *174*, 241–246.
(35) Diguna, L. J.; Qing, S.; Kobayashi, J.; Toyoda, T. *Appl. Phys. Lett.* **2007**, *91*, 23116/23111–23116/23113.
(36) Mora-Sero, I.; Gimenez, S.; Moehl, T.; Fabregat-Santiago, F.; Lana-Villareal, T.; Gomez, R.; Bisquert, J. *Nanotechnology* **2008**, 19.